Acta Biochim Biophys Sin, 2017, 49(12), 1058–1066
doi: 10.1093/abbs/gmx112
Advance Access Publication Date: 31 October 2017
Original Article

Original Article

Antimicrobial activity and mechanism of Larch bark procyanidins against *Staphylococcus aureus*

Xinchao Li[1], Congfen He[1], Liya Song[1], Ting Li[1], Shumei Cui[1], Liping Zhang[2], and Yan Jia[1,*]

[1]Beijing Key Laboratory of Plant Resources Research and Development, School of Science, Beijing Technology and Business University, Beijing 100048, China, and [2]MOE Key Laboratory of Wooden Material Science and Application, College of Materials Science and Technology, Beijing Forestry University, Beijing 100083, China

*Correspondence address. Tel: +86-10-68984937; E-mail: jiayan@btbu.edu.cn

Received 13 April 2017; Editorial Decision 21 July 2017

Abstract

Larch bark procyanidins (LBPCs) have not only antioxidant and antitumor properties, but also strong bacteriostatic effects. However, it is not clear about the antibacterial mechanisms of LBPC. In this work, the antibacterial effects and mechanisms of LBPC on *Staphylococcus aureus* were studied in the aspects of morphological structure, cell wall and membrane, essential proteins, and genetic material. The results showed that LBPC effectively inhibited bacterial growth at a minimum inhibitory concentration of 1.75 mg/ml. Bacterial morphology was significantly altered by LBPC treatment, with the cell walls and membranes being destroyed. Extracellular alkaline phosphatase content, bacterial fluid conductivity, and Na^+/K^+-ATPase and Ca^{2+}-ATPase activities in the membrane system were all increased. In the energy metabolic systems, the activities of succinate dehydrogenase, malate dehydrogenase, and adenosine triphosphatase (ATPase) were all decreased, resulting in a slowdown of metabolism and bacterial growth inhibition. Changes of protein content and composition in the bacteria suggested that the protein expression system was affected. In addition, LBPC was found to bind to DNA grooves to form complexes. Thus, LBPC has a very strong inhibitory effect on *S. aureus* and can kill *S. aureus* by destroying the integrity and permeability of the cell wall and cell membrane, affecting protein synthesis, and binding to DNA.

Key words: Larch bark procyanidins, *Staphylococcus aureus*, bacteriostatic mechanisms

Introduction

Larch bark (*Larix gmelinii*) is a deciduous tree of the genus *Larix* in the family Pinaceae [1]. It is a primary species in the coniferous forests of Northeast China and Inner Mongolia, and its bark is one of the most important forestry byproducts in China. Procyanidin (PC) extracted from Larch bark is a naturally active substance. Research on its structure has shown that PC is a polyphenolic compound [2] composed of (+)-catechin and (−)-epicatechin structural units and forms dimers linked at positions 4–8. Previous research on PC primarily focused on its extraction, purification, antioxidant properties, and stability. PC has strong 1,1-diphenyl-2-picrylhydrazyl (DPPH) free-radical scavenging and anti-lipid peroxidation capacities [3]; its antioxidant capacity is about several times of those of Vitamin C and Vitamin E [4,5], and it exhibits a good dose–effect relationship. PC stability negatively correlates with ambient temperature and pH. Studies of PCs derived from other sources [6–10] have revealed that this large category of substances have not only antioxidant and antitumor properties, but also strong bacteriostatic effects [11]. However, there are rare studies of the antibacterial effects and mechanisms of LBPC from different sources and with different structures.

Foodborne diseases caused by bacterial contamination are among the most important problems affecting human public health and food safety [12]. *Staphylococcus aureus* is an important pathogenic bacterium in human that can cause local purulent infections as well as pneumonia, osteomyelitis, and other systemic infections. Food contaminated by *S. aureus* not only undergoes decay and deterioration, but some strains can produce enterotoxins that result in food poisoning. *S. aureus*-induced food poisoning accounts for the majority of bacterial food poisoning cases.

Plant-derived antibacterial drugs are widely embraced because of their low toxic side effects. Addition of antibacterial materials extracted from plants to food, healthcare, and cosmetic products can provide antiseptic benefits as well as ensure their safety [13].

In this study, we systematically studied the effects of Larch bark procyanidins (LBPCs) on *S. aureus* morphological structure, cell wall and membrane, essential proteins, and genetic material, and elucidated the associated molecular mechanisms (targets and location). Our data provide a theoretical basis for new, safe, and effective natural preservatives for food, healthcare, and cosmetic products.

Materials and Methods

Experimental materials

Staphylococcus aureus (CGMCC 1.8721) was maintained in our own laboratory. LBPC was obtained from Beijing Forestry University (Beijing, China). Analytical-grade anhydrous ethanol, methanol, phenol, isoamyl alcohol, disodium phosphate, sodium chloride, chloroform and sodium dihydrogen phosphate, disodium hydrogen phosphate were purchased from Beijing Chemical Works (Beijing, China). Nutrient broth and nutrient agar were purchased from Beijing Aobox Biotechnology (Beijing, China). Alkaline phosphatase (AKPase) detection, Na^+/K^+-ATPase assay, and Ca^{2+}-ATPase assay kits were purchased from Nanjing Jiancheng Bioengineering Institute (Nanjing, China). Lysozyme, 1 M Tris-HCl, 0.5 M EDTA, and the SDS-PAGE preparation kit were purchased from Solarbio Life Sciences (Beijing, China).

Minimum inhibitory concentration determination

Nutrient agar containing a LBPC concentration gradient (1–2 mg/ml) was prepared. Selected *S. aureus* colonies were suspended in sterile saline and compared with the 0.5 McFarland turbidity standard (reagents were purchased from Beijing Chemical Works). Bacterial suspension (200 μl) was plated onto the nutrient agar plates and incubated for 12 h in a 37°C incubator. Bacterial growth was observed, and the minimum inhibitory concentration (MIC) was determined as the smallest dilution of LBPC in which bacteria did not grow.

The growth curve of *S. aureus* treated with LBPC

Nutrient broth was inoculated with *S. aureus* at a concentration of 1% (v/v). LBPC solutions of different concentrations were added separately into the bacterial culture to final concentrations of 1/2 MIC, 3/4 MIC, and 1 MIC. An untreated culture was used as a control. The cultures were incubated at 37°C with shaking at 180 rpm. The optical density (OD) at 540 nm of the samples was measured at different time points to establish the growth curves.

Scanning electron microscopic analysis of *S. aureus* treated with LBPC

S. aureus cells were collected and added to nutrient broth with or without 1 MIC of LBPC and incubated at 37°C with shaking at 180 rpm. Bacteria were collected by centrifugation at 12 and 24 h and fixed with glutaraldehyde (2.5% in phosphate buffer saline). Samples were dehydrated through a gradient of ethanol solutions, subject to critical-point drying, coated with gold, and observed for morphological and structural changes under a scanning electron microscope (Quanta200; FEI, Eindhoven, Netherlands).

Transmission electron microscopic analysis of *S. aureus* treated with LBPC

S. aureus was cultured as described in the previous section. Bacteria were collected by centrifugation after 12 and 24 h. The cell pellets were fixed with glutaraldehyde (2.5%) for 1 h and osmium (1%) tetroxide for 2 h, respectively, rinsed with 0.1 M phosphate buffer (pH = 7.4), and dehydrated through a gradient of ethanol solutions. Samples were soaked in a 1:1 mixture of ethanol/embedding solution for 2 h and then changed to pure embedding solution overnight. Then, the embedding solution was changed once and samples were embedded for 24 h. Ultrathin sections were stained and observed using a transmission electron microscope (JEM-1400; JEOL, Tokyo, Japan).

Determination of *S. aureus* extracellular AKPase activity treated with LBPC

Nutrient broth was inoculated with *S. aureus* at a concentration of 1% (v/v). LBPC solutions of different concentrations were added separately to the bacterial culture at final concentrations of 1/2 MIC and 1 MIC. Simultaneously, a negative control group was established. Bacteria were collected at different time intervals, washed with normal saline (sodium chloride solution) three times, centrifuged, and resuspended. Five microliters of bacterial suspension were collected for the measurement of extracellular AKPase activity using the AKPase detection kit as described previously [14].

Determination of *S. aureus* extracellular β-galactosidase content treated with LBPC

Bacteria were pretreated as described in the previous section. Bacterial suspension and *o*-nitrophenyl β-D-galactopyranoside (4%) were combined at a ratio of 20:1 (v/v), mixed thoroughly, and placed in a 37°C water bath. One milliliter of the reaction mixture was collected at different time intervals and centrifuged. The supernatants were collected and the absorbance at 420 nm was measured with a microplate reader (Infinite M200PRO, TECAN, Männedorf, Switzerland) to determine the extracellular β-galactosidase content.

Determination of the bacterial fluid conductivity treated with LBPC

Nutrient broth was inoculated with *S. aureus* at a concentration of 1% (v/v). LBPC solutions were added separately to the bacterial culture at final concentrations of 1/2 MIC and 2 MIC. A negative control was included. The cultures were incubated at 37°C with shaking at 180 rpm. The conductivity of the samples was measured at different time intervals (0, 30, 60, 90, 120 min) with a conductivity meter (KYE-100B; Fuma, Shanghai, China).

Determination of the Na^+/K^+-ATPase and Ca^{2+}-ATPase activity treated with LBPC

Nutrient broth was inoculated with *S. aureus* at a concentration of 1% (v/v). LBPC solution was added to the bacterial culture at a final concentration of 1 MIC. A negative control (bacterial culture without LBPC solution) was included. Bacteria were collected at different culture intervals, washed with normal saline three times, centrifuged, and resuspended. After cells were disrupted with an ultrasonic disrupter, the enzyme activities were measured using the Na^+/K^+-ATPase and Ca^{2+}-ATPase assay kits as described previously [14].

Determination of the SDH, MDH, and total ATPase activity treated with LBPC

Bacteria were pretreated as described in the previous section. The supernatant was collected after centrifugation. Succinate dehydrogenase (SDH), malate dehydrogenase (MDH), and total ATPase activities were measured using the corresponding assay kits as described previously [14].

Determination of the total protein expression in *S. aureus* treated with LBPC

S. aureus cells were treated with LBPC at 1 MIC for 6 h or 24 h and centrifuged at 16,099 *g* for 5 min at 4°C to pellet the cells. The cells were washed with phosphate buffer saline (PBS) three times, frozen overnight at –80°C, and freeze-dried in vacuum for 24 h. To every 100 mg dry weight of bacteria, 1 ml cell lysis buffer consisting of 8 M urea, 2 M thiourea, 4% (m/v) CHAPS, 60 mM DTT, and 1% PMSF was added and mixed by vortexing. After ultrasonic disruption, the lysate was centrifuged and the supernatant was collected for SDS-PAGE (12%) analysis and Coomassie blue staining.

Genomic DNA extraction

Bacterial solution (30 ml) was centrifuged at 2795 *g* for 10 min, and the pellets were resuspended in 500 µl TE (1 M Tris-HCl, pH 8.0, 0.5 M EDTA). Fifty microliters of lysozyme (20 mg/ml) was added into the cell suspension and incubated at 37°C for 60 min. Then, 50 µl of SDS solution (10%) and 20 µl of proteinase K (20 mg/ml) were added into the mixture and incubated at 37°C for another 1 h. After that, 10 µl of RNase A (10 mg/ml) was added and incubated at 37°C for 30 min. One hundred microliters of 5 M NaCl solution and 100 µl of CTAB (Cetyltrimethyl Ammonium Bromide)/NaCl solution were added, mixed well and heated at 65°C for 10 min. Finally, an equal volume of chloroform/isoamyl alcohol (24:1, v/v) was added, mixed well, agitated for 30 min, and centrifuged at 16,099 *g* for 5 min. The supernatant was collected and transferred to a new tube, and an equal volume of phenol/chloroform/isoamyl alcohol (25:24:1, v/v/v) was added, mixed well, and centrifuged at 11,180 *g* for 5 min. The supernatant was collected and two volumes of anhydrous ethanol was added, mixed well, allowed to settle for 10 min and centrifuged at 16,099 *g* for 5 min. The precipitate was collected, rinsed once with 70% ethanol, and dried at room temperature. TE was added to dissolve the DNA. DNA content and purity were measured with the microplate reader. The prepared genomic DNA was stored at –20°C.

Fluorescence experiment

To 100 µl of LBPC solution (4 mg/ml), 100 µl of *S. aureus* genomic DNA at different concentrations (0–0.8 mg/ml) was added and incubated in the dark at 37°C, 32°C, or 27°C for 1 h. Then, fluorescence was measured at an excitation wavelength of 280 nm and emission wavelengths of 310–500 nm with the microplate reader [15].

UV–vis spectroscopic measurement

To 100 µl of LBPC solution (4 mg/ml), 100 µl of *S. aureus* genomic DNA at different concentrations (0–0.8 mg/ml) was added and incubated in the dark at 37°C for 1 h. Then, samples were scanned at ultraviolet wavelengths from 230 to 450 nm with a spectrophotometer (Lambda 950, PerkinElmer, Waltham, USA) [15].

Effect of ion strength

To 100 µl of LBPC solution (4 mg/ml), 100 µl of *S. aureus* genomic DNA at different concentrations (0.2–0.8 mg/ml) was added to allow the formation of LBPC–DNA complex. Then, 100 µl of NaCl solutions of different concentrations (0–20 mg/ml) were separately added and the mixtures were incubated at 37°C for 1 h. Fluorescence was scanned at an excitation wavelength of 280 nm and emission wavelengths from 310 to 500 nm with the microplate reader.

Competitive experiment

DAPI (4′,6-diamidino-2-phenylindole)–DNA complex was prepared using 2 µg/ml DAPI and 0.20 mg/ml DNA. One hundred microliters of LBPC solutions of different concentrations (0–4 mg/ml) were added and the mixtures were incubated at 37°C for 1 h. Fluorescence was scanned at an excitation wavelength of 295 nm and emission wavelengths from 370 to 600 nm with the microplate reader.

Statistical analysis

Statistical significance was calculated by Student's *t*-test or analysis of variance (ANOVA) using SPSS Statistics 19.0.1. A statistical probability of $P < 0.05$ was considered significant.

Results

Establishment of the MIC

To study the antibacterial effect, MIC determination was performed. As shown in **Table 1**, turbidity of *S. aureus* was observed at LBPC concentrations of 1, 1.25, and 1.5 mg/ml, while no growth was observed at LBPC concentrations of 1.75 and 2 mg/ml. Thus, the MIC of LBPC on *S. aureus* is 1.75 mg/ml.

Effect of LBPC on *S. aureus* growth

To study the effect of LBPC on *S. aureus* growth, the growth curve (**Fig. 1**) was established. Compared with the control group, the optical density (OD) of the bacterial suspension was significantly decreased after LBPC treatment, suggesting that LBPC has inhibitory effects against *S. aureus*. Based on the growth curve, the growth of *S. aureus* was inhibited, and the number of bacteria was

Table 1. MIC of LBPC extract to *S. aureus*

Solution concentration (mg/ml)	1	1.25	1.5	1.75	2
bacteriostatic effect	–	–	–	+	+

Note: '–' represents no bacteriostatic effect, '+' represents a bacteriostatic effect.

significantly decreased. The inhibitory effect on *S. aureus* was increased with increasing concentration of LBPC, indicating that the effect of LBPC is dose-dependent within a certain range.

Effect of LBPC on *S. aureus* morphology

To study the effect of LBPC on *S. aureus*, morphology study was performed. The effect of LBPC (1.75 mg/ml) on *S. aureus* morphology is shown in **Fig. 2**. Scanning electron microscopy showed that the surface of control *S. aureus* was smooth and uninterrupted (**Fig. 2A–C**), whereas the surface of *S. aureus* treated with LBPC for 12 h showed clear vesication or irregular protruding structures (**Fig. 2D**). After 24 h of LBPC treatment, bacteria were surrounded by exudate, which may be cytoplasm extruded from the cells (**Fig. 2E**). Transmission electron microscopy showed clearly visible cell walls and membranes in untreated *S. aureus*, with regular and intact morphology (**Fig. 2F–H**), whereas after 12 h (**Fig. 2I**) and 24 h (**Fig. 2J**) of LBPC treatment, bacterial cell walls and membranes were slightly damaged.

Effect of LBPC on cell wall permeability

To study the effect of LBPC on cell wall permeability, AKPase activity was determined. Extracellular AKPase activity after LBPC treatment of *S. aureus* was shown in **Fig. 3A**. After LBPC treatment, the extracellular AKPase activity was increased continuously and was significantly higher than that of the control group. After 6 h, extracellular AKPase content in *S. aureus* treated with 1/2 MIC and 1 MIC of LBPC was increased to 1.8 folds and 3.1 folds, respectively, as compared to the control group. The substantial AKP leakage showed that the integrities of the bacterial cell walls and cell membranes were destroyed.

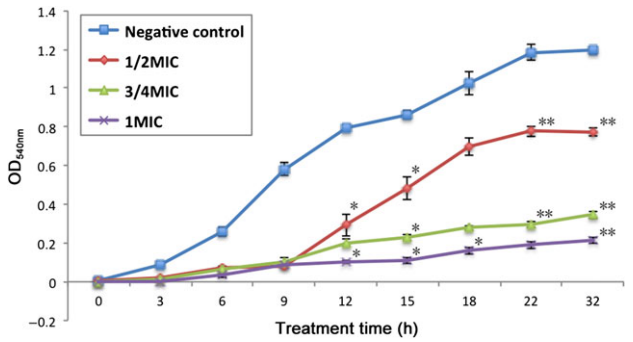

Figure 1. Effect of LBPC on the growth curve of *S. aureus* $^{*}P < 0.05$ and $^{**}P < 0.01$ indicated statistically significant differences of LBPC treatment vs. negative control calculated by SPSS statistics.

Effect of LBPC on cell membrane integrity

To study the effect of LBPC on cell membrane integrity, extracellular β-galactosidase content was determined. **Figure 3B** shows the extracellular β-galactosidase content in *S. aureus* after LBPC treatment. After 6 h of LBPC treatment, extracellular β-galactosidase content in cells treated with 1 MIC LBPC increased from 0.134 to 0.331 units/U, and the activity in cells treated with 1/2 MIC LBPC increased from 0.088 to 0.288 units/U. Both groups treated with LBPC exhibited significantly increased β-galactosidase content as compared to the control group, with fold increases of 6.01 and 5.2, respectively. These results demonstrated that LBPC damaged the cell membrane of *S. aureus*, leading to leakage of intracellular β-galactosidase.

Changes in bacterial fluid conductivity after LBPC treatment

To study the changes of permeability of the cell membrane, bacterial fluid conductivity was determined. **Figure 3C** shows the conductivity of bacterial fluid after the addition of LBPC. Bacterial fluid conductivity increased with LBPC treatment time. After treatment with 2 MIC LBPC for 120 min, bacterial fluid conductivity increased from 770 to 970 μs/cm, and after treatment with 1/2 MIC LBPC for 120 min, the conductivity increased from 765 to 941 μs/cm, showing increases of 25.9% and 23.0%, respectively. Both values were larger than those noted for controls. These results showed that LBPC increased the membrane permeability of *S. aureus*, leading to ion leakage.

Effect of LBPC on the activity of ion channel enzymes in the membrane system

To study the changes of permeability of the cell membrane, the change of activity of ion channel enzymes was investigated. **Figure 4A** shows the effect of 1 MIC LBPC on the activity of the membrane-

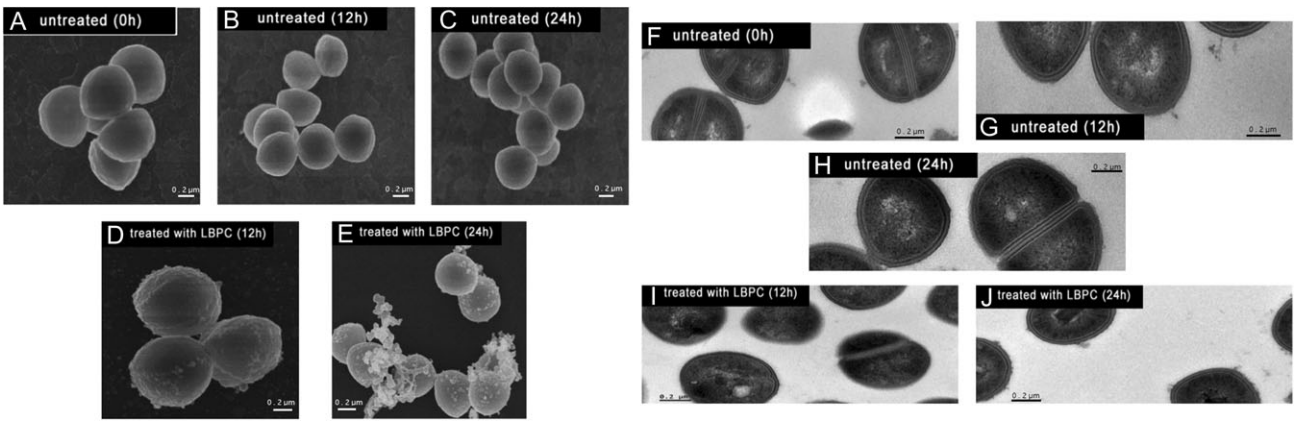

Figure 2. Scanning electron micrographs and transmission electron micrographs of *S. aureus* (A–E) Scanning electron micrographs: untreated at 0 h (A), untreated at 12 h (B), untreated at 24 h (C); treated with LBPC (1.75 mg/ml) for 12 h (D), treated with LBPC (1.75 mg/ml) for 24 h (E). (F–J) Transmission electron micrographs: untreated at 0 h (F), untreated at 12 h (G), untreated for at 24 h (H); treated with LBPC (1.75 mg/ml) for 12 h (I), treated with LBPC (1.75 mg/ml) for 24 h (J).

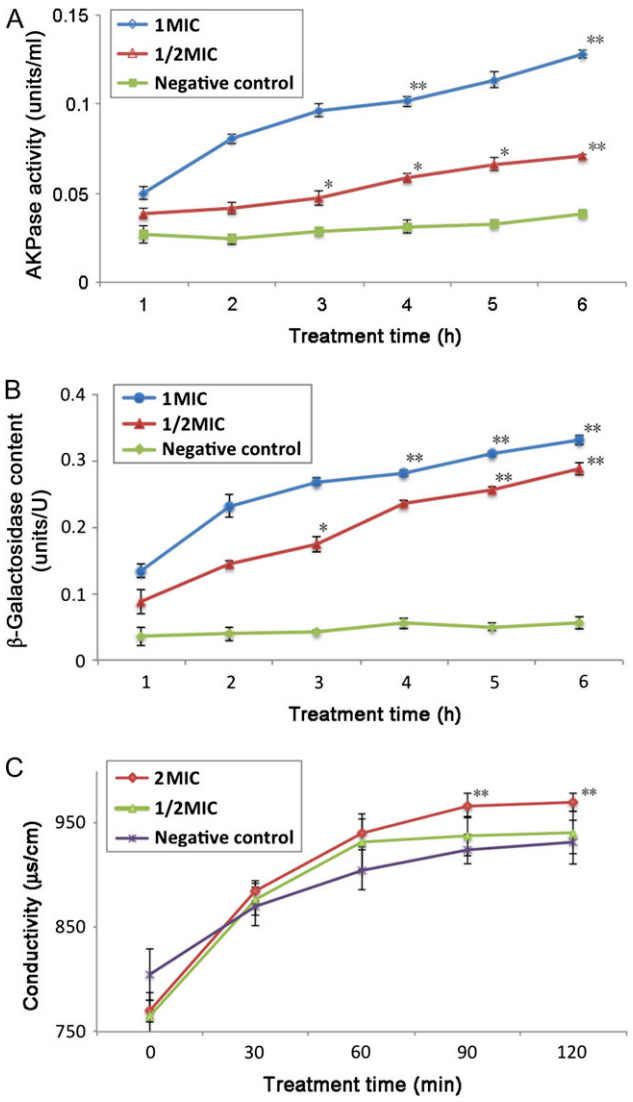

Figure 3. The effect of LBPC treatment on extracellular AKPase activity, β-galactosidase content and fluid conductivity (A) Extracellular AKPase activity in *S. aureus* after LBPC treatment. $*P < 0.05$ and $**P < 0.01$ indicated statistically significant differences of LBPC treatment vs. negative control. (B) Extracellular β-galactosidase content in *S. aureus* after LBPC treatment. $*P < 0.05$ and $**P < 0.01$ indicated statistically significant differences of LBPC treatment vs. negative control. (C) Bacterial fluid conductivity after LBPC treatment. $*P < 0.05$ and $**P < 0.01$ indicated statistically significant differences of LBPC treatment vs. negative control.

bound ion channel Na^+/K^+-ATPase in *S. aureus*. Na^+/K^+-ATPase activity was stably increased after 1 MIC LBPC treatment. After 6 h, Na^+/K^+-ATPase activity was increased from 0.003 mg protein/ml to 0.03 mg protein/ml. The enzymatic activity after 6 h of culture was 1.86-fold as that of the negative control. This result showed that LBPC activated membrane-bound ion channels in *S. aureus*, and that bacterial cells maintained cellular function by changing the ion concentrations inside and outside the cell membrane in order to resist the effects of the adverse environment. **Figure 4B** shows the effect of LBPC on the activity of the membrane-bound ion channel Ca^{2+}-ATPase. Ca^{2+}-ATPase activity in the group treated with 1 MIC LBPC showed a stably increasing trend. The enzymatic activity after 6 h of culture was 1.17-fold as that of the negative control. This finding supports that LBPC affects membrane-bound ion channels in *S. aureus*, and that the intracellular Ca^{2+} concentration increases with LBPC treatment, resulting in Ca^{2+}-ATPase stimulation in order to maintain low intracellular calcium concentration.

Effect of LBPC on the activity of essential energy metabolism enzymes in *S. aureus*

To study the effect of LBPC on the activity of essential energy metabolism enzymes in *S. aureus*, MDH, SDH, and ATPase activities were determined. As shown in **Table 2**, MDH, SDH, and ATPase activities were all decreased by LBPC treatment for 8 h. SDH activity decreased after 4 h of LBPC treatment, and the activity after 8 h of treatment was 14.47 U/mg protein, which was a decrease of 13.8% as compared to the control. In addition, ATPase activity in cells treated for 8 h and in control cells were 2.96 ± 0.21 U/mg protein and 3.21 ± 0.12 U/mg protein, respectively, indicating a decrease of 7.8% in the treated vs. control cells. Finally, MDH activity was decreased by 6.1% as compared to the negative control. These data show that bacterial energy metabolism is disrupted following LBPC treatment.

Effect of LBPC on total protein expression in *S. aureus*

To study the effect of LBPC on total protein expression in *S. aureus*, SDS-PAGE was performed. **Figure 5** shows the results of SDS-PAGE analysis of *S. aureus* treated with LBPC. The intensities of the protein bands at 35.0 and 66.2 kDa were increased after treatment, and new bands appeared, while some bands disappeared. Changes in the protein map were most apparent after 24 h of LBPC treatment, with changes in both total protein amount and of protein composition. This shows that LBPC has an effect on bacterial protein expression profile.

Effect of *S. aureus* genomic DNA on LBPC fluorescence intensity

To study the effect of LBPC on genetic material of *S. aureus*, the change of fluorescence intensity of *S. aureus* DNA treated with LBPC was explored. **Figure 6A** shows the fluorescence spectra of LBPC in the presence of different concentrations of *S. aureus* DNA. LBPC has a maximum emission peak at 400 nm (λ_{ex} = 280 nm). The maximum LBPC fluorescence emission peak was quenched in the presence of *S. aureus* genomic DNA, and the degree of quenching gradually increased with increasing concentration of genomic DNA. At the same time, the emission peak gradually blue-shifted. At a genomic DNA concentration of 0.8 mg/ml, the blue shift of the LBPC fluorescence peak was ~20 nm. These results showed that *S. aureus* genomic DNA may form a complex with LBPC.

Stern–Volmer curves of LBPC fluorescence quenching by *S. aureus* DNA at different temperatures

The quenching efficiency between a fluorescent molecule and a quencher is given by the following Stern–Volmer equation:

$$F_0/F = 1 + K_q\tau_0[Q] = 1 + K_{SV}[Q]$$

where F_0 is the fluorescence intensity of the fluorescent substance prior to addition of quencher, F is the fluorescence intensity of the fluorescent substance after treatment with quencher, K_q is the rate constant of the quenching process between the two molecules, τ_0 is the average fluorescence lifetime of the fluorescent molecule in the

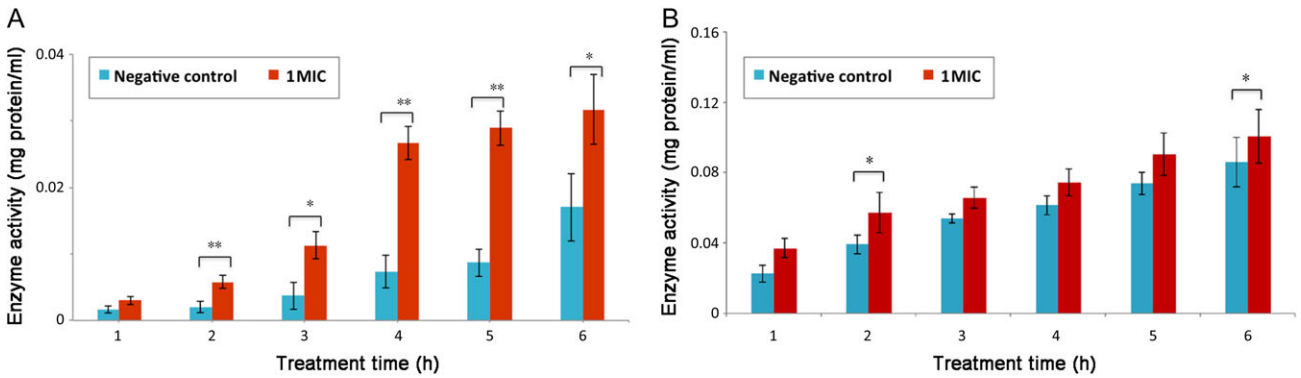

Figure 4. Effect of LBPC on Na^+/K^+-ATPase activity and Ca^{2+}-ATPase activity in *S. aureus* (A) Effect of LBPC on Na^+/K^+-ATPase activity. (B) Effect of LBPC on Ca^{2+}-ATPase activity. $*P < 0.05$ and $**P < 0.01$ indicated statistically significant differences of LBPC treatment vs. negative control calculated by SPSS.

Table 2. Effects of LBPC on the activity of key enzymes in energy metabolism of *S. aureus*

	Negative control		LBPC treatment	
	4 h	8 h	4 h	8 h
MDH activity (U/mg protein)	0.06 ± 0.02	0.06 ± 0.01	0.04 ± 0.02	0.06 ± 0.02
SDH activity (U/mg protein)	9.41 ± 2.12	16.79 ± 1.79	8.22 ± 1.53	14.47 ± 1.03
Total ATPase activity (U/mg protein)	2.38 ± 1.41	3.21 ± 0.12	1.36 ± 0.70	2.96 ± 0.21

absence of quencher (~10^{-8} for the majority of biological macromolecules), [Q] is the concentration of quencher, and K_{SV} is the Stern–Volmer constant, which shows the rate constant of the quenching process between the two molecules and the decay constant of a single molecule.

Figure 6B shows the Stern–Volmer curves of LBPC fluorescence quenching by *S. aureus* DNA at different temperatures. Within the range of the temperatures tested, the Stern–Volmer curves of LBPC quenching by *S. aureus* genomic DNA showed a good linear relationship without significant bias toward the *y*-axis, showing that the quenching of LBPC fluorescence by *S. aureus* DNA occurs through a quenching process [16].

Table 3 shows the Stern–Volmer constants for LBPC–*S. aureus* DNA complexes at different temperatures. With increasing temperature, the K_{SV} value of the complex decreased, and the fluorescence quenching rate constant K_q was far greater than the maximum diffusion collision quenching constant (2×10^{10} l mol^{-1} s^{-1}) of each type of quencher in the dynamic quenching process of biological macromolecules. This shows that a ground-state non-fluorescent complex is formed, and the fluorescence quenching mechanism is static quenching [17]. Thus, *S. aureus* genomic DNA forms a static complex with LBPC.

Effect of *S. aureus* genomic DNA on LBPC ultraviolet spectra

To study the effect of genetic material of *S. aureus* on LBPC, the change of ultraviolet spectra of LBPC treated with *S. aureus* DNA was investigated. **Figure 7A** shows the ultraviolet-visible absorption spectra of LBPC in the presence of various concentrations of *S. aureus* genomic DNA. With increasing DNA concentration, the absorbance of the LBPC solution gradually increased, exhibiting a hyperchromic effect. The hyperchromic effect is an obvious characteristic of non-covalent bonds, suggesting that the bond

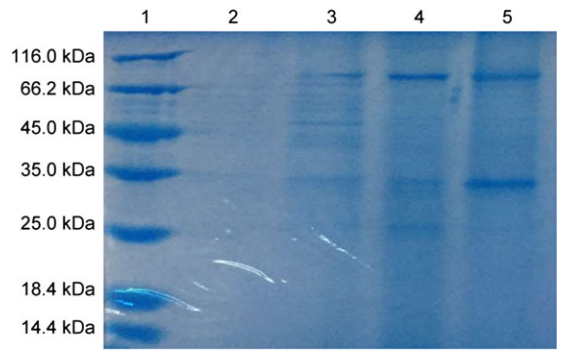

Figure 5. Effect of LBPC on the expression of intracellular total proteins of *S. aureus* Lane 1, protein marker; lane 2, *S. aureus* without LBPC for 6 h; lane 3, *S. aureus* without LBPC for 24 h; lane 4, *S. aureus* with LBPC for 6 h; lane 5, *S. aureus* with LBPC for 24 h.

between LBPC and *S. aureus* DNA is electrostatic or groove bonding [18].

Interaction pattern of LBPC with *S. aureus* DNA

To study the direction of LBPC interacting with *S. aureus* DNA, the effect of ion strength on the LBPC–DNA system was explored. **Figure 7B** shows the effect of ion strength on the LBPC–*S. aureus* DNA complex. Fluorescence intensity decreased with increasing NaCl concentration. These results are consistent with the ultraviolet-visible absorbance spectra, suggesting that LBPC and *S. aureus* DNA interact via groove or electrostatic bonding [19].

Figure 7C shows the effect of LBPC on the fluorescence intensity of the DAPI–*S. aureus* DNA complex. After addition of LBPC, the fluorescence intensity of the DAPI–DNA complex decreased significantly. At a LBPC concentration of 4 mg/ml, the fluorescence

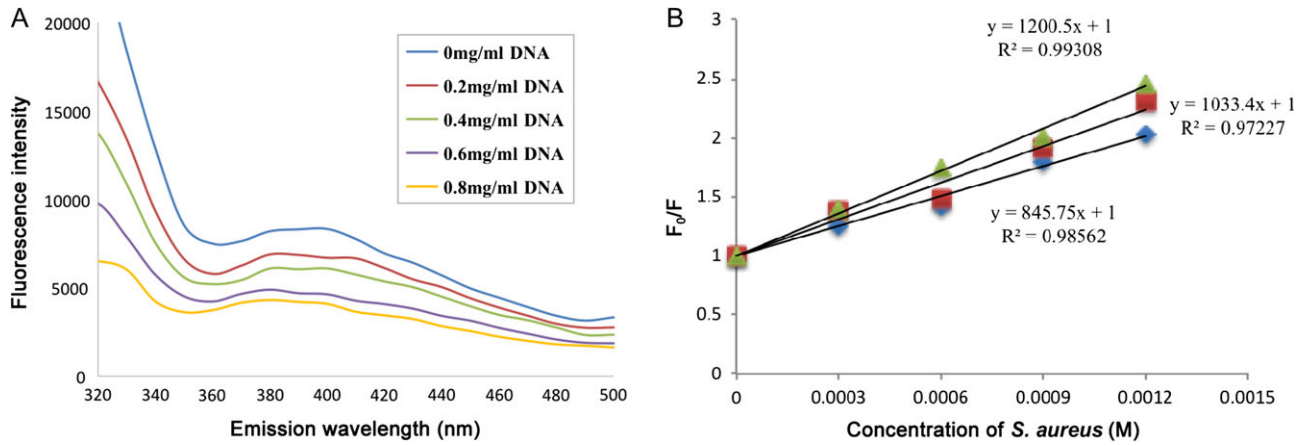

Figure 6. The effects of *S. aureus* DNA on LBPC fluorescence intensity (A) Fluorescence intensity of LBPC in the presence or absence of different concentrations of *S. aureus* DNA. The maximum LBPC fluorescence emission peak was quenched in the presence of *S. aureus* genomic DNA, and the degree of quenching gradually increased with increasing concentration of genomic DNA. The results showed that *S. aureus* genomic DNA may form a complex with LBPC. (B) Stern–Volmer curve of the effect of *S. aureus* DNA on LBPC fluorescence quenching at different temperatures.

Table 3. Stern–Volmer constant of LBPC–*S. aureus* DNA system at different temperatures

T (K)	K_{SV} (l mol^{-1})	K_q (l mol^{-1}s^{-1})	R^2
300.15	1.20×10^3	1.20×10^{11}	0.99308
305.15	1.03×10^3	1.03×10^{11}	0.97227
310.15	0.84×10^3	0.84×10^{11}	0.98562

intensity decreased by 41.98%, suggesting that LBPC can substitute DAPI and thus competes with DAPI at the *S. aureus* DNA binding sites. This binding effect between LBPC and *S. aureus* DNA is classified as groove binding, suggesting that LBPC can bind to the minor groove of the DNA double helix [20].

Discussion

LBPC exhibited effective bacteriostatic activity against *S. aureus*, even at low concentrations. Investigation of the underlying mechanism revealed that LBPC destroys the integrity and permeability of the cell wall and membrane, interferes with protein synthesis, engages in DNA groove binding, and disrupts normal physiological functions, leading to death.

The MIC of LBPC on *S. aureus* was determined to be 1.75 mg/ml, and the growth curve of *S. aureus* in the presence of LBPC intuitively reflected this inhibitory effect of LBPC on *S. aureus*. Within a certain concentration range, the inhibitory effect was positively correlated with the concentration of bacteriostatic agent. Scanning and transmission electron microscopy results showed that the surface of *S. aureus* treated with LBPC was damaged, with exudates surrounding the bacteria, and cell walls and membranes being interrupted and indistinct. With increasing treatment time, these phenomena were exacerbated, consistent with the conclusions drawn on the basis of the growth curves. To validate these observations and elucidate the underlying mechanism, we conducted a series of experiments to analyze the effects of LBPC on cell wall and membrane integrity, the enzymatic system, total protein, and DNA binding.

These results of cell wall and cell membrane integrity experiments showed that after LBPC treatment, extracellular AKPase content increased significantly over that in the control group, indicating AKPase leakage after LBPC treatment, and thus, that LBPC destroys the cell wall of *S. aureus* [21]. In addition, extracellular β-galactosidase content in treated *S. aureus* cells was higher than that in controls, showing that LBPC damages the cell membrane of *S. aureus* [22]. Meanwhile, bacterial fluid conductivity was increased after LBPC treatment, indicating increased membrane permeability and leakage of electrolytes such as K^+, Ca^{2+}, and Na^+. These results show that LBPC has a destructive effect on the permeability and integrity of the cell wall and cell membrane of *S. aureus*. These findings were consistent with the results of scanning and transmission electron microscopy. In addition, since AKPase regulates the metabolism of intracellular calcium ions [23], the substantial AKPase leakage after LBPC treatment suggests changes in intracellular calcium ion concentration and abnormalities in ion channels and related enzymes that regulate calcium ion concentration.

Na^+/K^+-ATPase is an important membrane protein that functions to maintain membrane permeability, an intracellular environment with low sodium and high potassium, and a resting potential. After LBPC treatment, Na^+/K^+-ATPase activity was stably increased. After 6 h of treatment, the activity of Na^+/K^+-ATPase on the *S. aureus* cell membrane was 1.86 times that of the negative control group. Likewise, in the presence of LBPC, the intracellular Ca^{2+} concentration was increased. Increased intracellular calcium concentration indicates activation of the Ca^{2+}-ATPase in the endoplasmic reticulum membrane and rapid transport of intracellular Ca^{2+} into the inner endoplasmic reticulum for storage. The Na^+/K^+-ATPase transport system facilitates Ca^{2+} efflux from the cell, thereby maintaining low intracellular Ca^{2+} concentration [24]. Because LBPC has a destructive effect on the bacterial membrane structure and function, it impedes *S. aureus* to balance intracellular and extracellular ion concentrations to maintain cellular activities. Under this condition, the cell is overloaded with calcium [25], which may increase the production of free radicals, damaging the structure and function of the energy metabolism system and leading to tissue and cell damage.

Our experiment results in the intracellular enzymatic systems corroborate with the above hypotheses. SDH is important for energy metabolism in microorganisms, and its activity is a sensitive indicator of damage to the energy metabolic systems [26]. MDH plays a

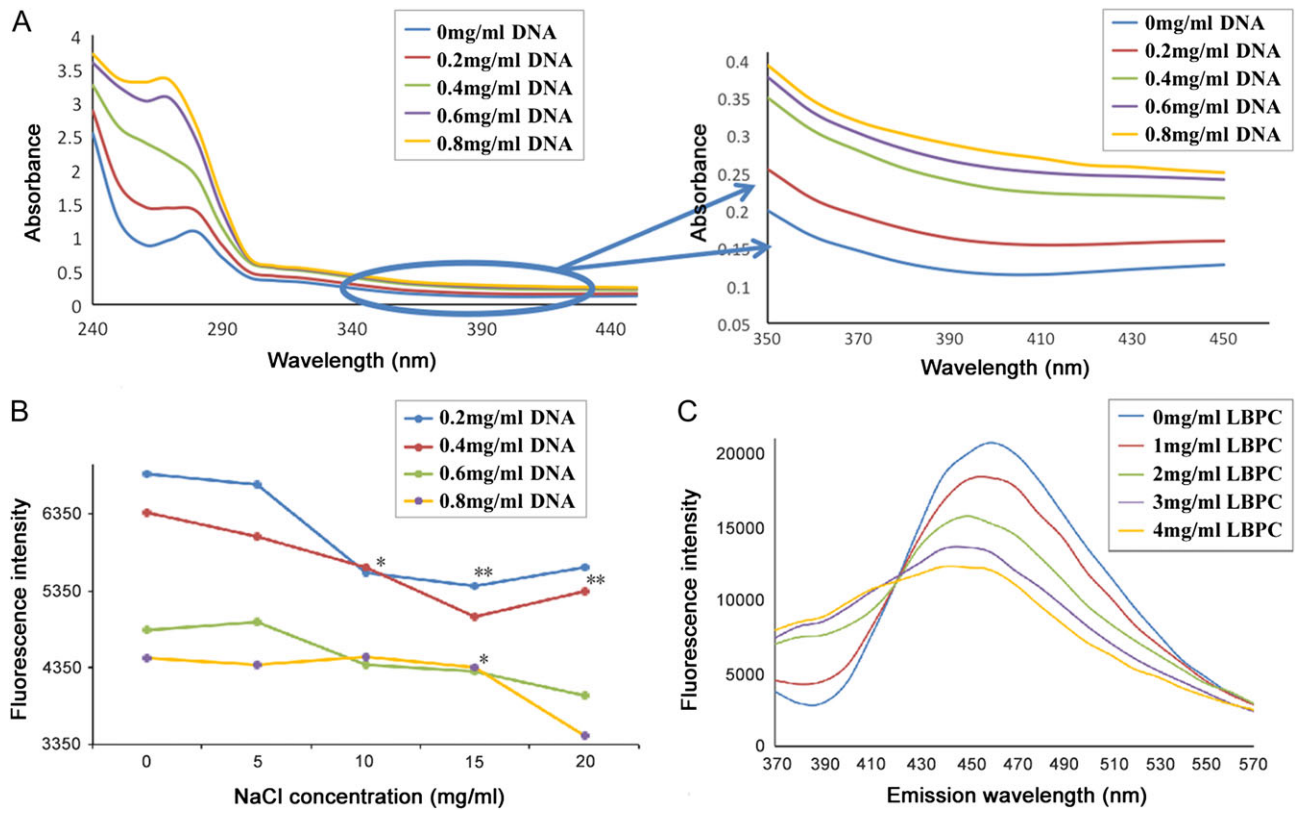

Figure 7. The interaction of LBPC and *S. aureus* DNA (A) Effect of *S. aureus* DNA on LBPC ultraviolet spectra. (B) Effect of NaCl on the interaction between *S. aureus* DNA and LBPC. $*P < 0.05$ and $**P < 0.01$ indicated statistically significant differences of NaCl treatment vs. negative control calculated by SPSS statistics. (C) Effect of LBPC on the binding of DAPI with *S. aureus* DNA. LBPC can substitute DAPI and thus competes with DAPI at the *S. aureus* DNA binding sites, suggesting that LBPC can bind to the minor groove of the DNA double helix.

crucial role in the tricarboxylic acid cycle of microorganisms, and is essential for cell growth, metabolism, and proliferation. Our data showed that LBPC has the greatest effect on SDH activity among the energy metabolism-related enzymes tested, with a decrease of 13.8% as compared to the control group. MDH activity and total ATPase also exhibited a decreasing trend. The activity of essential energy metabolic enzymes was decreased [27], thus interfering with energy metabolism systems, reducing metabolic rate and inhibiting bacterial growth. In addition, ATP production was also decreased [25] and the distribution of ions inside and outside the cell was abnormal, with Na^+ and Ca^{2+} accumulating inside the cells, which was consistent with results showing increased intracellular Ca^{2+} and Ca^{2+}-ATPase activity. In addition, SDS-PAGE analysis showed that LBPC treatment changed the protein content and composition in *S. aureus*, suggesting that LBPC might affect protein expression systems, thus inhibiting bacterial growth. The experimental results described above show that LBPC can interfere with the activity of essential metabolic enzymes in bacteria, affecting protein synthesis.

To study the binding effect of LBPC to *S. aureus* genetic material as well as the mode of interaction, fluorescence spectroscopy, ultraviolet spectroscopy, and other techniques were used. Fluorescence spectroscopy and Stern–Volmer curves showed that static quenching occurs between LBPC and *S. aureus* genomic DNA. Ultraviolet spectroscopy and ion strength studies confirmed that the mode of binding between LBPC and *S. aureus* genomic DNA is static binding or groove binding. Competitive analysis experiments further proved LBPC and DNA interact via groove binding.

In conclusion, LBPC has a strong inhibitory effect on *S. aureus*. Systematic research of the bacteriostatic mechanism showed that LBPC damages the integrity and permeability of the cell wall and cell membrane, affects membrane protein synthesis, and binds to the grooves of DNA, leading to *S. aureus* cell death. Apart from theoretical significance and application value, further elucidation of this mechanism would provide a rational basis for the use of LBPC as a natural preservative in food, healthcare, and cosmetic products.

Funding

This work was supported by the grants from the National Natural Science Foundation of China (Nos. 31501415 and 31401390), the Scientific Research Project of Beijing Educational Committee (No. SQKM201610011008), and the China Cosmetic Collaborative and Innovation Center, BTBU (No. 19008001060).

References

1. Jiang GQ. Study on the Fractionation, purification and catalyzed degradation of proanthocyanidins from larch bark. Northeast Forestry University, 2013.
2. Cui XX, Zhang XL, Tang HW, Zhang LP, Xu CH, Sun SQ. Study on extracts of active substances from Larch Bark by FTIR spectroscopy. *Specteosc Spectral Anal* 2012, 32: 1810–1814.

3. Zhang XL. Studies on antioxidant properties and structure of proanthocyanidins from larch bark. Beijing Forestry University, 2013.
4. Stevenson DE, Hurst RD. Polyphenolic phytochemical-just antioxidants or much more. *Cell Mol Life Sci* 2007, 64: 2000–2016.
5. García-Marino M, Rivas-Gonzalo JC, Ibáñez E, García-Moreno C. Recovery of catechins and proanthocyanidins from winery by-products using subcritical water extraction. *Anal Chim Acta* 2006, 563: 44–50.
6. Kang Y, Zhang JL, Shi XH, Zhang CJ. Effect of grape seed proanthocyanidins extract on TGF-βRII and Smad7 expression in human skin fibroblasts induced by ultraviolet A. *Chin J Dermatol Venerol Integ Trad W Med* 2015, 14: 341–343.
7. Sun Y, Xu BC, Gu WY. Anti-oxidization activity of grape seed proanthocyanin. *J Chin Cereals Oils* 2007, 22: 129–134.
8. Terra X, Pujadas G, Arola L, Biay M. Inhibitory effects of grape seed procyanidins on foam cell formation in vitro. *J Agric Food Chem* 2009, 57: 2588–2594.
9. Wang W, Chen JH, Wang XN, Li Q, Chen Q, Jiang JW. Grape seed proanthocyanidins induce apoptosis and autopha gic cell death in human hepatoma HepG2 cells. *J Jinan Univ* 2011, 32: 181–187.
10. Dong B, Diao TJ, Li YL, Li DM, Fu YM. The inhibitory effect of grape seed proanthocyanidins on *Candida albicans* in vitro. *Chin J Microecol* 2015, 27: 49–51.
11. Dong XM, Han RF, Liu TM. Antibacterial mechanism of grape seed proanthocyanidins against. *Food Ind* 2015, 36: 188–192.
12. Xu ZB, Liu XC, Li L, Li B. Development of *Staphylococcus aureus* enterotoxin in food-borne bacteria. *Mod Food Sci Technol* 2013, 29: 2317–2324.
13. Liu X, Zhang MS, Zhang C, Liu C. Angiotensin converting enzyme (ACE) inhibitory, antihypertensive and antihyperlipidaemic activities of protein hydrolysates from *Rhopilema esculentum*. *Food Chem* 2012, 134: 2134–2140.
14. Li T, Yang SR, Chen M, Song LY, He CF. Study on antibacterial mechanism of Ginger Magnolia bark extract against *Escherichia coli* and *Staphylococcus aureus*. *Mod Food Sci Technol* 2016, 32: 84–92.
15. Su BD, Liao LM, Lei GD, Wang B. Study on mechanism of the interaction of emodin and DNA. *J Instrum Anal* 2011, 30: 600–606.
16. Kalaivania P, Prabhakaran R, Kaveri MV, Huang R, Staples RJ, Natarajan K. Synthesis, spectral, X-ray crystallography, electrochemistry, DNA/protein binding and radical scavenging activity of new palladium (II) complexes containing triphenylarsine. *Inorg Chim Acta* 2013, 405: 415–426.
17. Zaitsev EN, Kowalczykowski SC. Binding of double-stranded DNA by *Escherichia coli* REcA protein monitored by a fluorescent dye displacement assay. *Nucleic Acids Res* 1998, 26: 650–654.
18. Shahabadi N, Kashanian S, Khosravi M, Mahdavi M. Multispectroscopic DNA interaction studies of a water-soluble nickel(II) complex containing different dinitrogen aromatic ligands. *Trans Met Chem* 2010, 35: 699–705.
19. Sun YT, Zhang HQ, Bi SY, Zhou XF, Wang L, Yan YS. Studies on the arctiin and its interaction with DNA by spectral methods. *J Luminescence* 2011, 131: 2299–2306.
20. Liu BM, Bai CL, Zhang J, Dong BY, Zhang YT, Liu B. In vitro study on the interaction of 4,4-dimethylcurcumin with calf thymus DNA. *J Luminescence* 2015, 166: 48–53.
21. Hara S, Yama K. Moricin. A novel type of antibacterial peptide isolated from the silkworm, *Bombyx mori*. *J Biol Chem* 1995, 270: 29923–29927.
22. Shen SX, Zhang TH, Yuan Y, Lin SY, Xu JY, Ye HQ. Effects of cinnamaldehyde on *Escherichia coli* and *Staphylococcus aureus* membrane. *Food Control* 2015, 1: 196–202.
23. Ivanvski S. Expression of bone matrix protein mRNAs by primary and cloned cultures of regenerative phenotype of human periodontal fibroblasts. *J Dent Res* 2001, 80: 1665–1671.
24. Endo J, Sano M, Katayama T, Hishiki T, Shinmura K, Morizane S, Matsuhashi T, *et al*. Metabolic remodeling induced by mitochondrial aldehyde stress stimulates tolerance to oxidative stress in the heart. *Circ Res* 2009, 105: 1118–1127.
25. Gulcan H, Ozturk IC, Arslan S. Alterations in antioxidant enzyme activities in cerebrospinal fluid related with severity of hypoxic ischemic encephalopathy in newborns. *Biol Neonate* 2005, 88: 87–91.
26. Piasecka M, Wenda RL, Ogofiski T. Computerized analysis of cytochemical reactions for dehydrogenases and oxygraphic studies as methods to evaluate the function of the mitochondrial sheath in rat spermatozoa. *Andrologia* 2001, 33: 1–12.
27. Jiang Y, Wang H. Observation on the activity of MDH of CWDM. *Guizhou Med J* 2001, 10: 893–894.